CHARACTERIZATION OF INGOT MATERIAL FOR SRF CAVITY PRODUCTION

J. Mondal[#], K.C. Mittal, Accelerator & Pulse Power Division, BARC, Mumbai,
G. Ciovati, P. Kneisel, G.R. Myneni, Jefferson Lab, Jefferson Ave, Newport News, VA , U.S.A.

Abstract

In recent years, large-grain/single-crystal niobium has become a viable alternative to the standard fine grain (ASTM grain size>6), high purity (RRR ≥ 250) niobium for the fabrication of high-performance SRF cavities for particle accelerators. In this contribution we present the results of a systematic study of the superconducting properties of samples obtained from four Niobium ingots (from CBMM, Brazil) of different purity. Measurements of bulk magnetization, surface pinning, critical temperature and thermal conductivity have been carried out on the samples subjected to different surface treatments such as buffered chemical polishing (BCP), 600^0C heat treatment, and low temperature baking (LTB). A correlation has been established between the LTB and the ratio $\frac{H_{c3}}{H_{c2}}$. In addition, the phonon peak in the thermal conductivity data is suppressed by the presence of trapped magnetic vortices in the samples.

INTRODUCTION

Niobium is the material of choice for superconducting radio frequency (SRF) cavity programs in different particle accelerator laboratories because of its mechanical properties favorable for formability, machining and also high T_C and high first flux penetration field H_{C1}.SRF cavity performances have been continually improved for past three decades to achieve reproducible quality factor of 10^{10} and E_{acc} field of 30-35MV/m. The present approach for the fabrication of superconducting radio frequency (SRF) cavities is to roll and deep draw sheets of polycrystalline high-purity niobium. Jefferson Laboratory pioneered the use of large-grain/single-crystal Nb directly sliced from an ingot for the fabrication of single-crystal high-purity Nb SRF cavities[1]. The large grain/single crystal niobium has several potential advantages over the polycrystalline niobium as discussed in Ref. [2] and has become a viable alternative to the standard fine grain (ASTM grain size>6), high purity (RRR ≥ 250) niobium for the fabrication of high-performance SRF cavities for particle accelerators. In this contribution we present the results of a systematic study of the superconducting properties of samples obtained from four Niobium ingots (from CBMM, Brazil) of different purity. The RF superconducting properties of the samples can later be tested in a TE_{011} coaxial cavity described in Ref. [3].

[#]jmondal@barc.gov.in

DESCRIPTION OF SAMPLES

Four samples were made from four different niobium ingots received from CBMM, Brazil. The Ingots named A, B, C and D have different RRR and different impurity contents. Samples are cut by wire EDM and then machined by lathe to a diameter of 6 mm and 120mm length. After machining, all the samples were degreased in ultrasonic bath with micro solution for 30 min. Table 1 shows the different surface treatments on the samples before each measurement.

Table 1: Surface treatments on samples A, B, C and D before each measurement. The number following the letter in the sample codes identifies the measurement number.

Measurement	Sample Code	Process
1st Set	A1,B1,C1,D1	BCP(1:1:1) to remove about 180 µm.
2nd Set	A2,B2,C2,D2	Degassed at 600^0C for 10 h at a vacuum $<10^{-6}$ Torr. Then degreased and BCP (1:1:2) to remove about 24 µm.
3rd Set	A3,B3,C3,D3	Degreased and baked at 100^0C for 12 hour at a vacuum $< 10^{-6}$Torr.
4th Set	A4,B4,C4,D4	BCP (1:1:2) 10 µm and baked at 120^0C for 12 hour at a vacuum $< 10^{-6}$Torr.
5th Set	A5,B5,C5,D5	BCP (1:1:2) 10 µm and baked at 140^0C for 12 hour at a vacuum $< 10^{-6}$

A system to measure the magnetization curve, thermal conductivity, the penetration depth and the surface pinning characteristics of the sample rod was designed and built. The system details are described in [3].

THERMAL CONDUCTIVITY AND EFFECT OF TRAPPED FLUX

Measurement of Thermal Conductivity and Evaluation of RRR

The thermal conductivity as a function of the average temperature of the sample is calculated using Fourier's law where the power supplied to the heater, *P*, the temperature difference, ΔT, the distance *d* between the two Cernox thermometers, and the cross-sectional area of the sample *A* are measured:

$$\kappa = \frac{P}{\Delta T}\frac{d}{A} \qquad (1)$$

The heater power and the sample temperature are controlled with a LakeShore 332 Temperature Controller. The RRR of the sample is defined by RRR = α K_S (4.2K), where α is the experimentally measured parameter and is defined by,

$$\alpha = \frac{\rho_{295K}}{R(y)L_0T} \qquad (2)$$

where ρ_{295K} = 14.4x10^{-7}Ω*cm is the resistivity at room temperature, L_0 = 2.45×10^{-8} W*K^{-2} is the Lorentz Constant and $y = \Delta(T)/k_BT$, Δ(T) being the BCS gap energy at the temperature T.
R(*y*) is the ratio of the electrons' contribution to the thermal conductivity in the superconducting state, k_{es} , divided by the electrons' contribution in the normal conducting state, k_{en}:

$$\kappa_{es} / \kappa_{en} = R(y) \qquad R(y) \le 1 \qquad (3)$$

R(*y*) can be calculated using the BCS theory and is equal to 0.311 at 4.2 K, using $\Delta(T)/k_BT_c$=1.76. The calculated value of α is equal to 4.5 at 4.2 K Experimentally measured value of α are 4.2,4.2, 4.3 and 4.5 respectively for B2,A2,C3 and D2. This is in good agreement with the theoretically calculated value of $\tilde{\alpha}$.

Figure 1 and figure 2 shows the experimental thermal conductivity curves in the range 1.8K-5K for 1st and 2nd set of measurements and the RRR values calculated by using Eqn.(2). The error in the experimental data is +/- 6%.

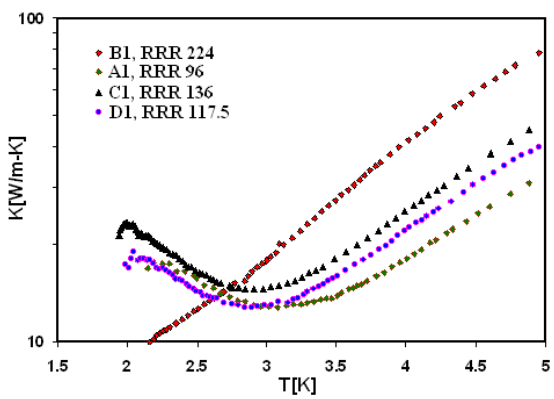

Figure 1: Thermal conductivity after 180 µm BCP.

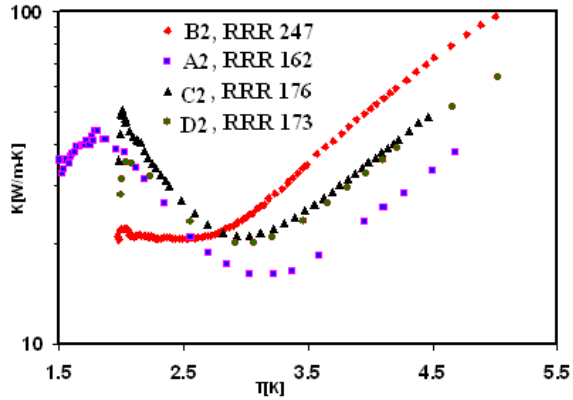

Figure 2: Thermal conductivity after 600^{0}C for 10 hour heat treatment at a vacuum <10^{-6} Torr followed by BCP(1:1:2) etching.

A cavity made of large grain or single crystal niobium operating below 2 K may have a better thermal stability due to the reduction of phonon scattering by grain boundaries (causing the so-called "phonon-peak"). The total heat conductivity of the superconducting metal is obtained by adding the electronic term k_{es}(T)and the and the lattice term $k_{latt,s}$(T) and a theoretical model described in [5] gives the following expression,

$$K_s(T) \cong R(y)\left[\frac{\rho_{295K}}{L \cdot RRR \cdot T} + A \cdot T^2\right]^{-1} + \left[\frac{1}{\exp(y)DT^2} + \frac{1}{BlT^3}\right]^{-1} \qquad (4)$$

In order to obtain k_s (T) using this model, it is necessary to give experimental values to three variables: temperature T, residual resistivity ratio RRR and the phonon mean free path l. The values of the fitted parameters A, B, and D are in good agreement with the theoretical values in ref. [5]. One such fit with the experimental data is shown in Figure 3.

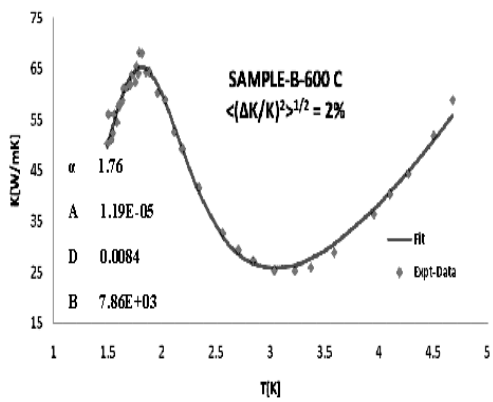

Figure 3: Fit of thermal conductivity data with Equation (4).

This fit was done taking into account the phonon mean free path as the sample thickness of 2 mm. In these studies we found that the phonon peak is clearly pronounced and it is enhanced after the 600^{0}C degassing.

Effect of Trapped Vortices on the Thermal Conductivity

The thermal conductivity measurement before applying a magnetic field to the sample shows clearly a phonon peak. After cycling the applied magnetic field from zero to above H_{C2} and then back to zero, the thermal conductivity measurements do not show the phonon peak anymore. If the sample temperature is raised above T_C and then lowered below T_C, with no magnetic field applied, then the phonon peak reappears in the thermal conductivity measurement. This clearly indicates that the trapped vortices from the remnant magnetization of the samples act as significant scattering centers to phonons. Figure 4 shows a typical measurent of thermal conductivity and the effect of trapped magnetic vortices. Figure 5 shows the thermal conductivity plotted as a function of magnetic field measured at 2K. The curve designated as Meissner state was measured before applying any magnetic field and other one is with the remnant magnetization, after cycling the applied field above H_{C2}. Figure 5 clearly shows that the thermal conductivity at 2 K is greatly reduced by the additional scattering of the phonons with the vortex cores.

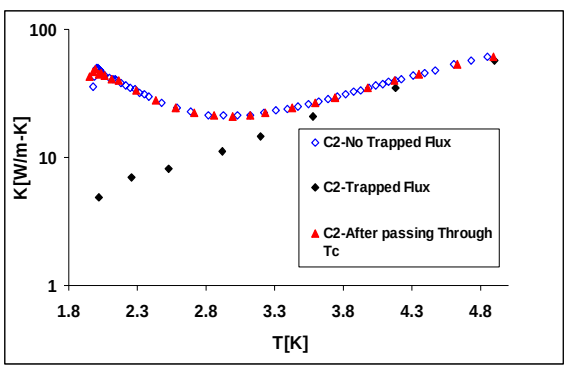

Figure 4: Thermal conductivity and effect of trapped flux.

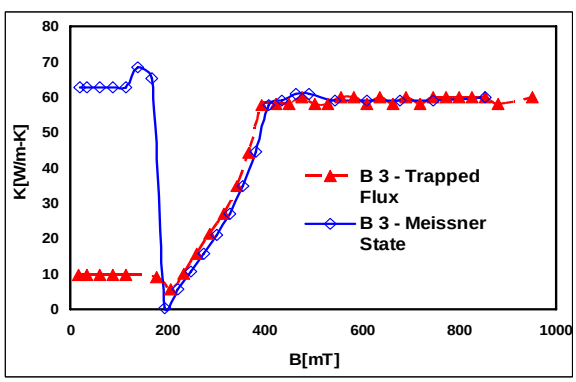

Figure 5: Thermal conductivity Vs Magnetic field with and without trapped flux.

MAGNETIZATION MEASUREMENT

Bulk Magnetization

The measurement of DC magnetization provides the first flux penetration value H_{C1}, the upper critical magnetic field H_{C2} and from M-H curve the thermodynamic critical field H_C is calculated. Pinning of vortices leads to irreversible magnetization curves. Figures 6 and 7 show the bulk magnetization curves for the 1st and 2nd set of measurements. The results show that H_{C1} and H_{C2} are not affected by the 600^{0}C heat treatment. The thermodynamic critical field is given by,

$$H_C^2 = 2\mu_0 \int_0^{H_{C2}} M(H)dH \qquad (5)$$

Table 2: DC Magnetization Measurement Results for 1st and 2nd Set of Samples

Sample	$B_{C1,2K}$(mT)	$B_{C2,2K}$(mT)	$B_{C,2K}$(mT)
A	172	400	184
B	181	388	186
C	175	410	184
D	176	405	189

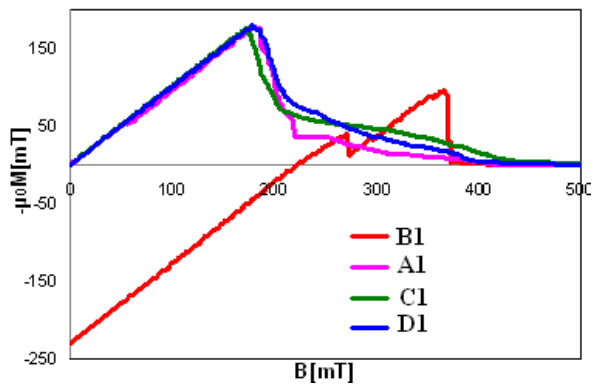

Figure 6: Magnetization curves of BCP samples at 2K.

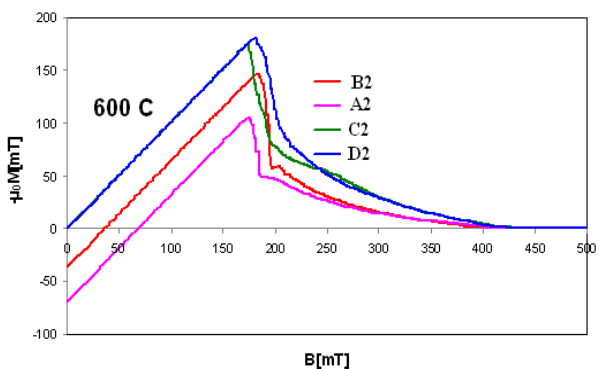

Figure 7: Magnetization curve of 600^{0}C heat treated samples at 2K.

The behaviour of the magnetization curve of sample B1 in Figure 6 shows strong paramagnetic characteristics but after 600^{0}C heat treatment the paramagnetic behaviour is

reduced but still present. Sample A2 in Figure 7 also show remnant magnetization at zero field. But for sample A2 t before the measurement at 2K, one set of measurement has carried out at 4.2 K which didn't show any remnant magnetization. As discussed in thermal conductivity section the remnant magnetization prevails from the 4.2K measurement in case of sample A2. But the strong paramagnetic behaviour of sample B1 is not clearly understood.

The magnetization curves in Figure: 6 of the sample C1, D1 and in Figure: 7 C2, D2 doesn't reach to zero above H_{C2} is due to the zero time offset of the magnetic field of the superconducting solenoid during ramp-up period. The offset value in all those curves from the zero level is about 5-7 mT. Also the linear fit of magnetic field as function of time in Figure: 8 shows a zero point offset of 6 mT.

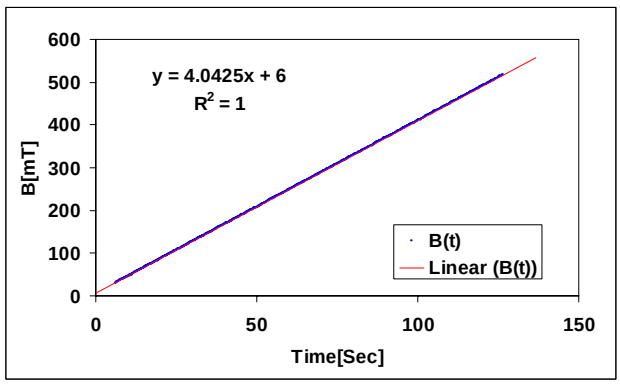

Figure 8: Ramp-up of magnetic field with time.

Surface Pinning

By connecting the pick-up coil around the sample rod as part of a L-C oscillator, it is possible to measure the changes of the penetration depth as a function of the applied DC magnetic field by measuring the changes of the oscillator's resonant frequency $f0$ (the base frequency is 270 kHz, sampling up to a depth ~10 □m) while slowly ramping up and down the magnetic field above H_{C3}.

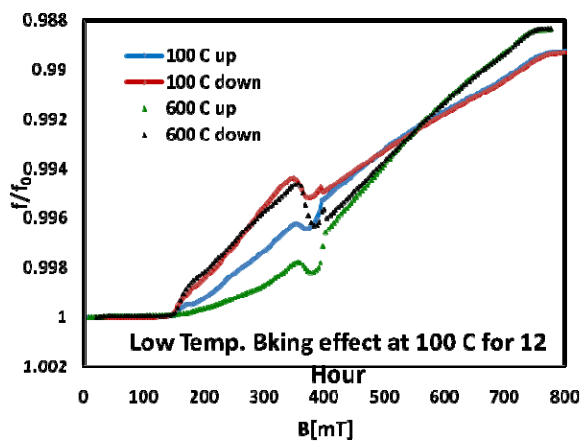

Figure 9: Surface pinning characteristics before and after the LTB.

This method provides information about surface pinning and allows measuring the surface critical field B_{C3}.The irreversibility of the curve between B_{C1} and B_{C2} is an indication of surface pinning. Figure 9 shows the typical behaviour of surface pinning measurements. The value of the surface H_{C1} and H_{C2} remains constant with different surface treatments like BCP 180 μm, 600 C 10 hr. heat treatment and 100 C, 120 C, bake for 12 hr. in vacuum. But H_{C2} starts to increase after 140 C baking. The data show that after low temperature baking the irreversibility reduces by a significant fraction. This can be interpreted as a reduction of impurities near the metal surface. Similar pinning measurements at higher frequency would allow reducing the sampling depth and therefore would have higher sensitivity to impurities within the penetration depth in the superconducting state.

Effect of LTB on Hc3/Hc2 Ratio

Theoretical model:

In real superconductor (SC) the surface is contaminated by impurities, dislocations, grain boundaries etc. which decreases the mean free path (mfp). In Shmidt's model [6] the surface of the bulk SC is represented by a film of thickness 'd' with GL parameter k_1 and the bulk SC is represented by k_2. The basic assumption in this model is that the surface layer and the bulk SC have the same T_C and H_C. This model predicts that the ratio of H_{C3}/H_{C2} is enhanced when $\boldsymbol{d \le \xi_0}$ and is given by the following relation,

$$\frac{H_{C3}}{H_{C2}} = 1.67\left[1+\left(\frac{k_1-k_2}{k_1}\right)\sqrt{1.7}\,\frac{d}{\xi(T)}\right] \qquad (6)$$

In order to apply this model in the region $T<<T_C$ it is required to take into account the nonlinearity of the microscopic theory. In this regard Hu and Korenman(HK) [7] derived the H_{C3}/H_{C2} ratio in the range $0 \le T \le T_C$ using Gorkov's gap equation. The ratio is given by,

$$\frac{H_{C3}}{H_{C2}} = 1.69C(t) \qquad (7)$$

where,

$$C(t) = 1 + 0.614(1-t) - 0.577(1-t)^{3/2} - 0.007(1-t)^2 + 0.106(1-t)^{5/2}$$

and $t = \dfrac{T}{T_C}$.

We apply Shmidt's model by multiplying Eq. (6) by HK polynomial C(t) in order to extend its validity to $T<<T_C$. The final form of the equation which has been used to explain the experimental results is given by,

$$R = \frac{H_{C3}}{H_{C2}} = 1.67C(t)\left[1 + \left(\frac{k_1 - k_2}{k_1}\right)\sqrt{1.7}\,\frac{d}{\xi(T)}\right] \quad (8)$$

The temperature dependence of H_{C3}/H_{C2} has two independent sources. One which takes into account the nonlinearity of the microscopic theory and the other consider the effect of the surface film of thickness 'd'.

k_2 is calculated using the relation $H_{C2} = \sqrt{2}k_2 H_c$, where H_{C2} is the experimentally measured value and Hc is calculated using Eqn. (5)

and ξ[T] is calculated by using the relation $H_{C2} = \frac{\phi_0}{2\pi\mu_0\xi^2}$.

Experimentally we measure the frequency as a function of applied magnetic field as discussed in the surface pinning measurement section. Since the contaminated surface layer thickness $d \le \xi_0$, so the vortices azimuthally collapse with each other when the surface critical field reaches $H_{C2,\ surf}$ value. As a result the change in penetration depth is very small and hence the transition at $H_{C2,\ surf}$ is not sharp enough to detect from the measured curve as shown in Figure 9. For the calculation of k_1 i.e. for the surface layer $H_{C2,\ surf}$ was determined by $H_{C2,\ surf} = H_{C3}/1.67*C(t)$[8]. Since the basic assumption on the above model is that both the surface layer and the bulk superconductor has the same thermodynamic critical field H_C an T_C, so k_1 is evaluated using $H_{C2,\ surf}$ value.

Experimental Results:

The experimental results are tabulated in the Table 3. The result shows that with the increased baking temperature the contaminated layer thickness increases to an average of 5.8 nm, 9.5 nm and 19.6 nm at 100 C, 120 C, and 140 C baking temperature respectively. But at 140 C both the contaminated layer thickness and bulk H_{C2} increases which may be due to the partial dissociation of the Nb_2O_5 layer as explained in the oxygen diffusion model [9]. The oxygen diffusion model corresponds to a diffusion depth of 7.6nm, 19nm and 40 nm for a baking at 100 C, 120 C and 140 C for 12 hour duration. Except for the 100 C bake the experimentally derived surface layer thickness is about half of the oxygen diffusion depth calculated by the theoretical model.

Also the first flux penetration i.e B_{C1} increases with the 100 C and 120 C baking for 12 hr. in vacuum. But it falls to 100 mT at 140 C baking.

Table 3: Results of low temperature baking studies measured at 2K

Sample	$B_{C1,surf}$ (mT)	$B_{C2,surf}$ [mT] Calculated	$B_{C3,surf}$ [mT]	R	d_{expt} [nm]
BCP(1:1:1) 180 μm					
A1	100	403	761	2.0	5.61
B1	120	372	703	1.93	7.35
C1	115	394	745	2.0	5.87
D1	104	378	714	1.98	5.46
600 C 10 Hour Degassing at a vacuum < 10-6 Torr then BCP(1:1:2) removing about 24 μm					
A2	115	398	752	2.02	6.84
B2	122	379	716	2.01	8.45
C2	118	384	725	1.98	6.66
D2	113	379	717	2.01	9.44
Low temperature baking at 100 C in a vacuum <5x10-7 Torr for 12 Hour					
A3	117	413	780	2.14	12.5
B3	113	395	746	2.15	13.8
C3	117	429	810	2.15	11.6
D3	111	408	772	2.2	16.7
Low temperature baking at 120 C in a vacuum <5x10-7 Torr for 12 Hour					
A4	129	410	774	2.1	14.5
B4	130	383	724	2.12	18.7
C4	130	407	770	2.1	14.6
D4	131	403	762	2.17	21.4
Low temperature baking at 140 C in a vacuum <5x10-7 Torr for 12 Hour					
A5	100	615	1162	2.76	30.1
B5	100	518	979	2.60	28.5
C5	100	595	1124	2.60	25.3
D5	104	556	1050	2.55	25.8

PENETRATION DEPTH & T_C MEASUREMENT

Penetration depth measurement as a function of temperature with different surface treatments provides qualitative information about the changes in the surface. Figure 10 shows how the change in penetration depth (Δλ) depends on the parameter y = $1/\sqrt{\left[1-(T/T_C)^4\right]}$. The slope of λ(y) represents the penetration depth at 0 K in the two-fluid model. As the LTB temperature is increased the slope of $d\lambda/d\,y$ decreases till 120^{0}C. At 140^{0}C baking the slope $d\lambda/d\,y$ increases at a faster rate resulting in a dirtier surface with decreased mean free path (mfp). In 100 and 120 C the slope continuously decreases meaning that diffusion of surface impurities toward the bulk and dilution of impurity concentration. The faster increase of the slope at 140 C might be due to the partial Nb_2O_5 layer dissociation and thereby

increasing the impurity concentration at the surface resulting in a lower mfp. The surface magnetization measurement further corroborates this fact as the bulk H_{C2} starts increasing at 140 C baking.

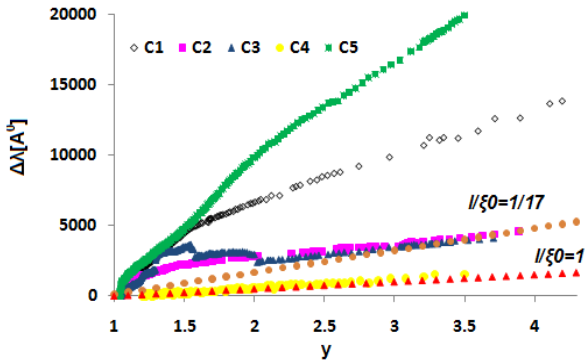

Figure 10: Δλ(y) measured on sample C after different surface treatments.

BCS theory predicts that Δλ as a function of y is linear. The present measurement shows that the dependence is not quite linear. All the measurements show that the Δλ – y characteristics have two slopes one at lower temperature (~7K) and the other at higher temperature. As discussed in Ref. [10] the general equation of penetration depth λ (T) for all values of mfp l and taking into account the random scattering is given by,

$$\lambda = \pi\left\{\int_0^{\infty} \ln\left[1+q^{-2}K(q)\right]dq\right\}^{-1} \qquad (9)$$

Where *K (q)* is obtained from the Fourier transform of the current density,

$$j(q) = -\left(\frac{c}{4\pi}\right)K(q)a(q) \qquad (10)$$

where *a (q)* is the Fourier component of the vector potential. Intuitively from our experimental Δλ(y) measurement it can be said that the condition $l \le \xi_0$ is satisfied as shown in Figure10. The theoretical Δλ –y curves are plotted for $l \le \xi_0$ as described in Ref.[10].The theoretical curves clearly shows that the mfp increases from 100^0C to 120^0C baking and reaching close to l= ξ_0. But these fits deviates at around y = 1.5 with a nonlinear slope till y =1 and deviation is large in BCP, 140 C surface treatments compare to other surface treatments like 600 C degassing, 100 and 120 C baking. As explained by Miller in Ref. (10) this deviation is determined by the parameter $2l/\pi\xi_0$ and lower the value of this parameter higher is the deviation in λ from the linear fit in the range of y = 1 to 1.5. The baking at120 C do not show any such nonlinear behaviour in the range of y = 1 to 1.5.This qualitatively implies that the initial surface impurities diffuses towards the bulk and addition of impurities due to the Nb_2O_5 dissociation is negligibly small and hence this increases the mfp which in turn reduces the nonlinearity in the penetration depth curve.

SUMMARY AND CONCLUSIONS

Thermal conductivity measurements on the four large-grain samples cut from Nb ingots of different purity show a phonon peak at about 1.9 K, except for the sample of highest purity (sample B). One important observation is that the phonon peak is eliminated by the presence of large amount of trapped magnetic flux, mainly due to the interaction between the phonons and the bound excitations in the vortices' core. The bulk properties of the samples such as T_C, B_C, H_{C1} and H_{C2} were essentially unchanged with surface treatments such as BCP, LTB. Surface pinning measurement shows that the H_{C3} value increases with the increased LTB temperature. It also shows that the surface H_{C1} is lower than the bulk H_{C1} and that the highest surface Hc1 was obtained after baking at 120°C for 12h. The irreversibility between Hc1 and Hc2 decreases significantly with the low temperature baking, thus a reduction in the surface pinning centers can be inferred. The ratio of H_{C3}/H_{C2} increases with the increased LTB temperature. The data has been analyzed with the Schmidt's model taking into account the low temperature correction to H_{C3}/H_{C2} ratio. The enhanced H_{C3}/H_{C2} ratio has been interpreted as the increased contaminated surface layer thickness. This fact is further corroborated by the penetration depth measurement.

ACKNOWLEDGEMENTS

This work was supported by US DOE contract DE-AC05-84ER40150 and Reference Metals Company Inc. CRADA 2004-S002-Mod 2.

REFERENCES

[1] P. Kneisel, G.R. Myneni, G. Ciovati, J. Sekutowicz, T. Carneiro, Proc of the 2005 Particle Accelerator Conference,Tennessee, paper TPPT076.

[2] P. Kneisel, Proc of the 13th SRF Workshop, Peking Univ, China, October 2007, paper Th102.

[3] G. Ciovati, J. Mondal, P. Kneisel, G.R. Myneni, M. Morrone, R. Bundy, B. Clemens, T. Elliott, G. Slack, L. Turlington, Proc of the 13th SRF Workshop, Peking Univ, China, October 2007, paper TuP01.

[4] "Theory of the thermal conductivity of superconductors", J. Bardeen, G. Rickayzen and L. Tewordt, Phys. Rev. 113, 982 (1959).

[5] F Koechlin and B Bonin, "Parametrization of the niobium thermal conductivity in the super conducting state", Supercond. Sci. Technol. 9, 453-460, (1996) [4] D.K. Finnemore and D.E. Mapother, Phys. Rev. 140 No. 2A (1965) 507.

[6] V.V.Shmidt, in Physical Metallurgy, Physical Chemeistry and Metals Physics of Superconductors,p.90 (Moscow: Nauka, in Russian 1967).
[7] C.Hu and V.Korenman, Phys. Rev. 185, 672(1969).
[8] S. Casalbuoni, E.-A. Knabbe , J. Koetzler , L. Lilje , L. von Sawilski , P. Schmueser , B. Steffen, Nucl. Instrum. Meth. A538, 45-64, (2005).
[9] G.Ciovati, Appl. Phys. Lett 89, 022507(2006).
[10] P.B.Miller, Phy.Rev, 113, 1209 (1959).